

IUCrJ

Volume 6 (2019)

Supporting information for article:

X-ray diffraction data as a source of the vibrational free energy contribution in polymorphic systems.

Phillip Miguel Kofoed, Anna Agnieszka Hoser, Frederik Diness, Silvia Capelli and Anders Østergaard Madsen

	W_5	W_100	W_125	W_150	W_175	W_200	W_RT
Chemical formula	C ₁₀ H ₈ Cl ₂ O ₆	C ₁₀ H ₈ Cl ₂ O ₆	C ₁₀ H ₈ Cl ₂ O ₆	C ₁₀ H ₈ Cl ₂ O ₆	C ₁₀ H ₈ Cl ₂ O ₆	C ₁₀ H ₈ Cl ₂ O ₆	C ₁₀ H ₈ Cl ₂ O ₆
M_r	295.08	295.08	295.08	295.08	295.08	295.08	295.08
Crystal system, space group	Triclinic, <i>P</i> -1	Triclinic, <i>P</i> -1	Triclinic, <i>P</i> -1	Triclinic, <i>P</i> -1	Triclinic, <i>P</i> -1	Triclinic, <i>P</i> -1	Triclinic, <i>P</i> -1
Temperature (K)	5	100	125	150	175	200	294
<i>a</i>, <i>b</i>, <i>c</i> (Å)	9.8021 (4), 7.7322 (4), 10.4934 (5)	9.8043 (4), 7.7484 (4), 10.5027 (5)	9.8090 (4), 7.7577 (3), 10.5083 (5)	9.8127 (2), 7.76700 (16), 10.5170 (3)	9.8178 (2), 7.77841 (17), 10.5270 (3)	9.8231 (2), 7.79072 (17), 10.5376 (3)	9.8461 (3), 7.84791 (19), 10.5783 (3)
α, β, γ (°)	116.848 (4), 124.3970 (4), 88.7890 (3)	116.731 (4), 124.349 (4), 88.853 (3)	116.688 (5), 124.329 (5), 88.869 (4)	116.638 (2), 124.323 (3), 88.869 (2)	116.595 (2), 124.299 (3), 88.884 (2)	116.557 (2), 124.277 (3), 88.896 (2)	116.412 (3), 124.159 (3), 88.976 (2)
<i>V</i> (Å³)	555.15 (1)	557.98 (1)	559.65 (4)	561.46 (2)	563.58 (2)	565.79 (2)	575.36 (3)
<i>Z</i>	2	2	2.0	2.0	2.0	2.0	2
Radiation type	Mo <i>K</i> α	Mo <i>K</i> α	Mo <i>K</i> α	Mo <i>K</i> α	Mo <i>K</i> α	Mo <i>K</i> α	Mo <i>K</i> α
μ (mm⁻¹)	0.60	0.60	0.60	0.60	0.59	0.59	0.58
Crystal size (mm)	2.0 × 0.5 × 0.35	2.0 × 0.5 × 0.35	2.0 × 0.5 × 0.35	2.0 × 0.5 × 0.35	2.0 × 0.5 × 0.35	2.0 × 0.5 × 0.35	2.0 × 0.5 × 0.35
Diffractionmeter	Bruker SMARTAPEX2 a rea detector	SuperNova, Single source at offset, Eos	SuperNova, Single source at offset, Eos	SuperNova, Single source at offset, Eos	SuperNova, Single source at offset, Eos	SuperNova, Single source at offset, Eos	SuperNova, Single source at offset, Eos
Absorption correction	Multi-scan SADABS2014/4	Multi-scan CrysAlis PRO, SCALE3 ABSPACK	Multi-scan CrysAlis PRO, SCALE3 ABSPACK	Multi-scan CrysAlis PRO, SCALE3 ABSPACK	Multi-scan CrysAlis PRO, SCALE3 ABSPACK	Multi-scan CrysAlis PRO, SCALE3 ABSPACK	Multi-scan CrysAlis PRO, SCALE3 ABSPACK
<i>T</i>_{min}, <i>T</i>_{max}	0.647, 0.748	0.473, 1.000	0.549, 1.000	0.534, 1.000	0.586, 1.000	0.586, 1.000	0.574, 1.000
No. of measured, independent and observed [$> 2.0\sigma(I)$] reflections	24786, 7048, 6026	96497, 5428, 4931	20138, 2810, 2564	65857, 5858, 5141	66140, 5867, 5015	66436, 5848, 4866	62436, 6432, 4511
<i>R</i>_{int}	0.039	0.050	0.039	0.041	0.042	0.042	0.049
($\sin \theta/\lambda$)_{max}(Å⁻¹)	0.927	0.856	0.691	0.880	0.882	0.880	0.880
<i>R</i>[$F^2 > 2\sigma(F^2)$], <i>wR</i>(F^2), <i>S</i>	0.027, 0.077, 1.47	0.023, 0.055, 1.30	0.023, 0.051, 1.18	0.025, 0.057, 1.26	0.027, 0.059, 1.26	0.028, 0.062, 1.29	0.037, 0.080, 1.35
No. of reflections	7048	5428	2810	5858	5867	5848	6432
No. of parameters	195	195	195	195	195	195	195
No. of restraints	16	16	16	16	16	16	16
$\Delta\rho_{max}$, $\Delta\rho_{min}$(e Å⁻³)	0.68, -0.93	0.45, -0.37	0.26, -0.38	0.34, -0.49	0.36, -0.42	0.36, -0.41	0.42, -0.48

White form

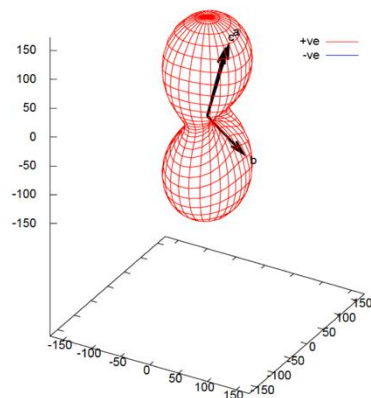
		Direction			
Axes	α (MK ⁻¹)	$\sigma\alpha$ (MK ⁻¹)	a	b	c
X ₁	-14.0733	1.0337	0.0128	0.9381	0.3461
X ₂	51.4334	3.3494	0.7531	0.6490	0.1077
X ₃	172.6677	7.7985	0.1192	-0.4907	0.8631
V	214.9940	12.0275			

Expansivity Indicatrix

The indicatrix has units of MK⁻¹.

Rotate +x Rotate -x Rotate +z Rotate -z
Down X₁ Down X₂ Down X₃ Value X:30

Value Z:60



Yellow form

		Direction			
Axes	α (MK ⁻¹)	$\sigma\alpha$ (MK ⁻¹)	a	b	c
X ₁	22.0416	0.1326	-0.9609	-0.2094	0.1811
X ₂	43.3472	0.9798	0.6159	-0.4444	0.6505
X ₃	94.5403	0.5836	0.3214	0.7465	0.5827
V	162.0085	1.8874			

Expansivity Indicatrix

The indicatrix has units of MK⁻¹.

Rotate +x Rotate -x Rotate +z Rotate -z
Down X₁ Down X₂ Down X₃ Value X:30

Value Z:60

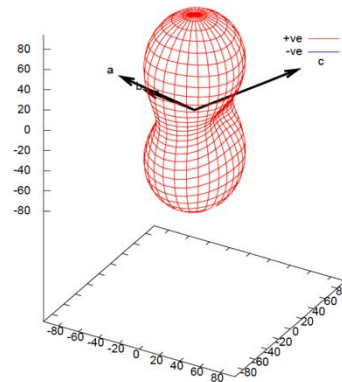


Figure S1. Expansivity indicatrices calculated by the PASCAL software. (Cliffe & Goodwin, 2012) Left: White form. Right: Yellow form.

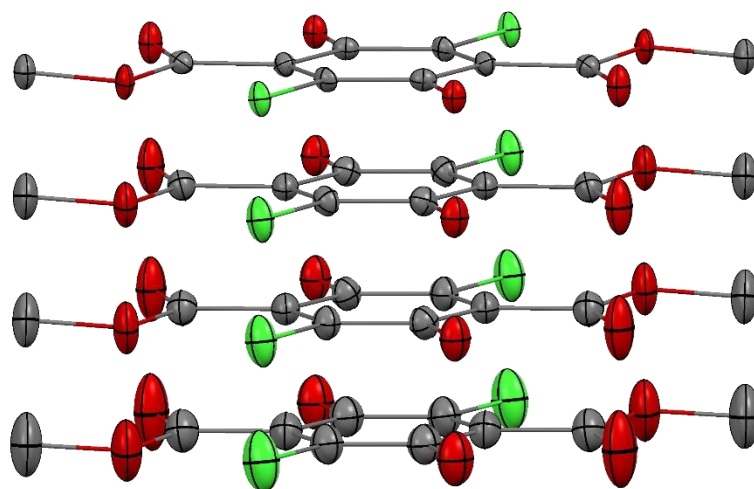


Figure S2. ADPs obtained by Dunitz and co-workers for Y polymorph

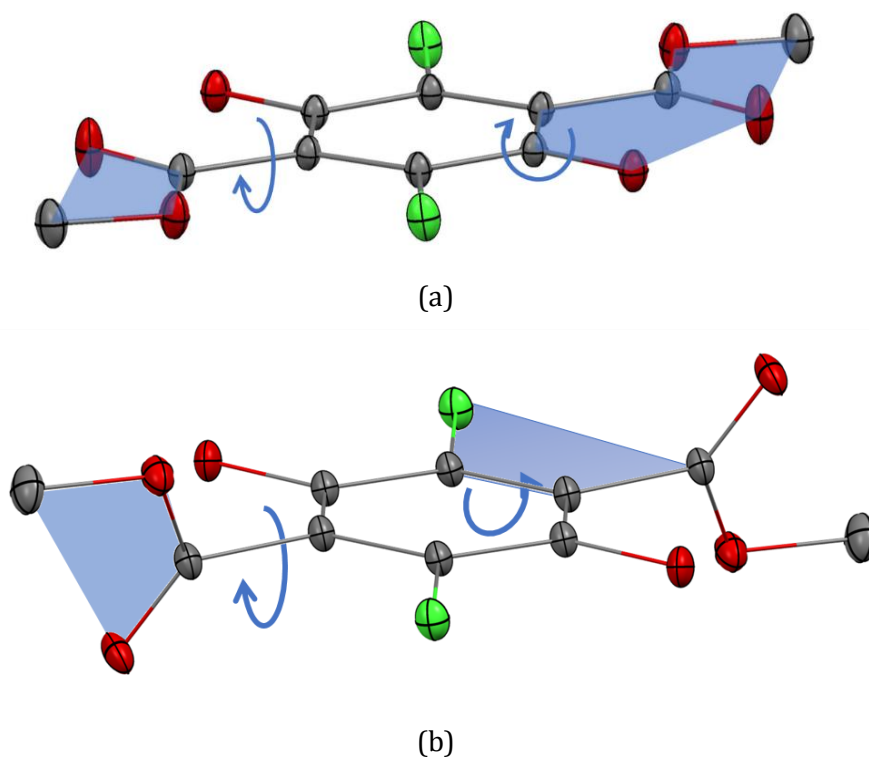


Figure S3. Description of internal vibrational modes in NKA models for yellow (a) and white (b).

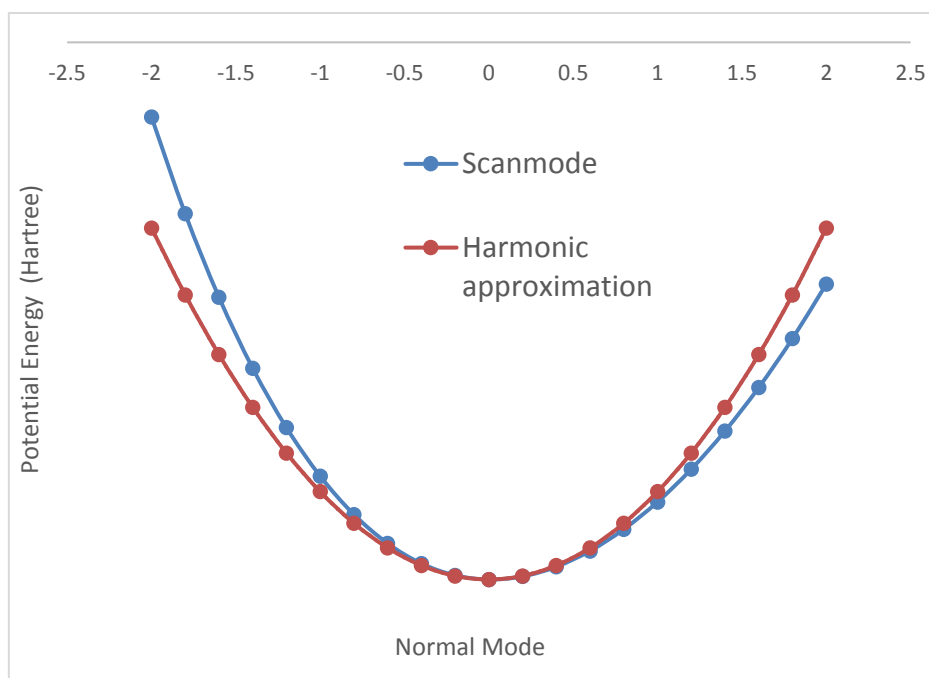
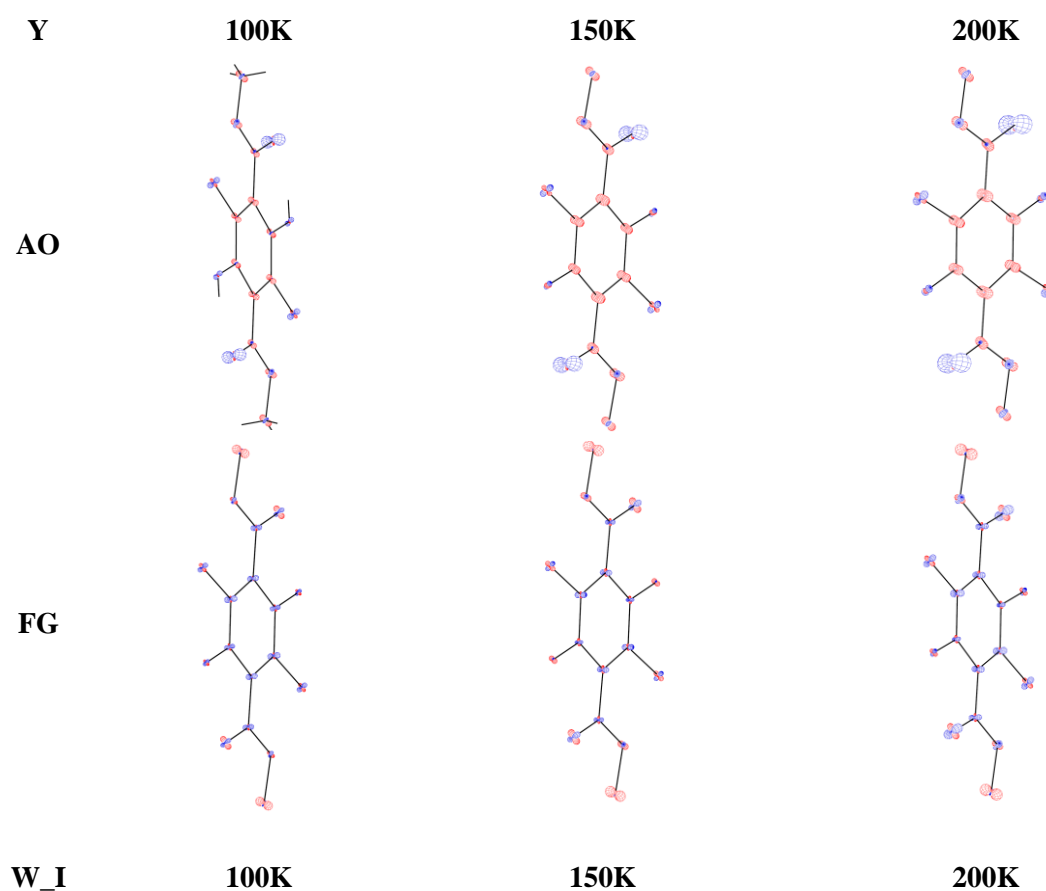
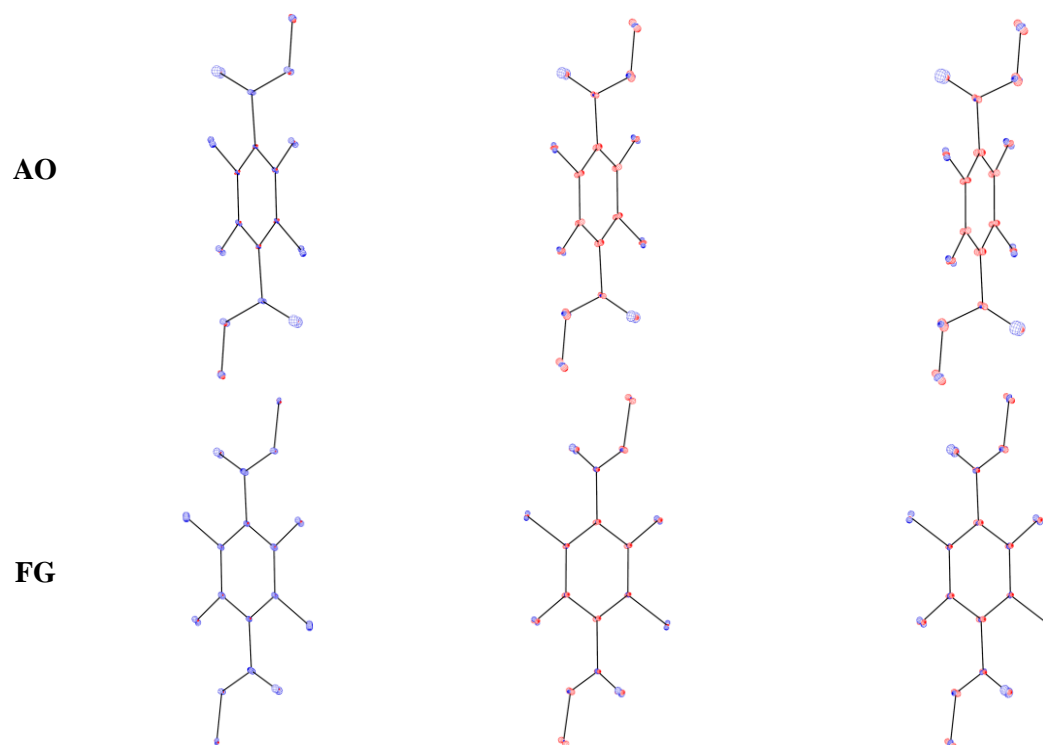


Figure S4. Energy scan along normal mode vector for Y, mode number 5.

Figure S5. PEANUT plots – difference between models from *NoMoRe* and from routine X-ray refinements (*Scaling applied in PEANUT 3.08*).





W_II 100K

150K

200K

AO

FG

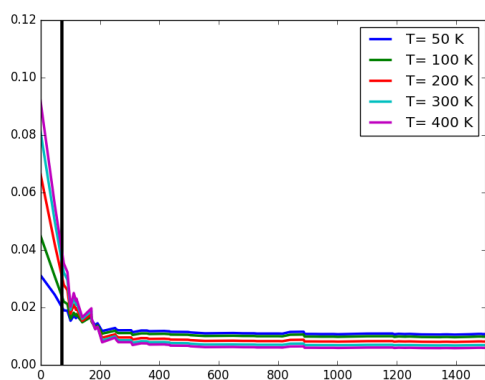
Table S2. Final statistics and frequencies obtained for yellow and white after NKA refinement

Polymorph	Model	Statistics after refinement: Observations/Restraints/Parameters R2ij	Frequencies (cm ⁻¹)	Gruneisen parameters	Main Eigenvector components
Yellow	TLS+ gruneisen+ internal_modes (see Fig S2a)	756 / 39 / 82 R2ij: 0.084	35 (1) 48 (1) 76 (7) 47 (2) 49 (2) 37 (1)	7.0(3) 5.0(8) 6.2(8) 5.0(2)	54% Lx + 46% Ly 95% Lz 45% Lx + 50% Ly + 5% Lz Tx Ty 50% Tz + 50% U1
White Molecule 1	TLS+ gruneisen+ internal_modes (see Fig S2b)	756 / 39 / 80 R2ij: 0.078	36(1) 53(2) 79(7) 35(1) 33(1) 48(2)	7.1(6) 4.7(8)	27% Lx + 73% Ly 5% Lx + 92% Lz 68% Lx + 25% Ly + 8% Lz 85% Tx + 13% Ty 14% Tx + 84% Ty 63% Tz + 16% U1 + 20% U2
White Molecule 2	TLS+ gruneisen+ internal_modes (see Fig S2b)	756 / 39 / 81 R2ij: 0.076	65(2) 58(2) 35(1) 36(1) 32(1) 51(2)	5.1(8) 5.7(6)	35% Lx + 32% Ly + 32% Lz 37% Lx + 61% Lz 28% Lx + 65% Ly 83% Tx + 5% Ty + 9% Tz + 3% U1 6% Tx + 93% Ty 9% Tx + 71% Tz + 14% U2 + 3% U1

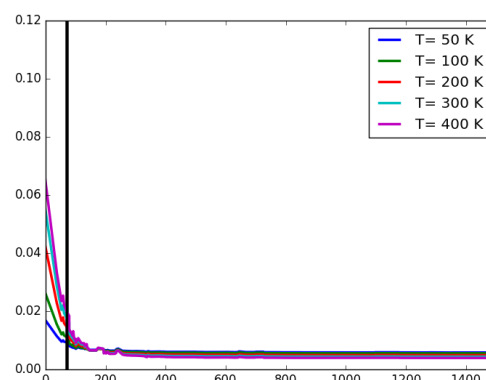
U1 = Butterfly motion; U2 = COO group rotation

Table S3. Energies computed for Y and W from supercell and Γ point DFT computations.

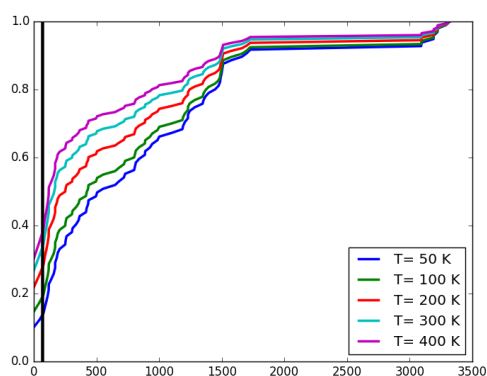
300K	E_Y	E_Y	E_W	E_W
	Supercell	Γ	supercell	Γ
$E_{total}/\text{kJ}\cdot\text{mol}^{-1}$	-4611791	-4611779	-9223583	-9223566
$E_{electronic}/\text{kJ}\cdot\text{mol}^{-1}$	-4612228	-4612213	-9224447	-9224419
$ST/\text{kJ}\cdot\text{mol}^{-1}$	85,8	77,5	177,6	176,9
$ZPE/\text{kJ}\cdot\text{mol}^{-1}$	476,5	470,3	947,5	938,2
$H_{vib}/\text{kJ}\cdot\text{mol}^{-1}$	45,3	41,4	93,5	91,9



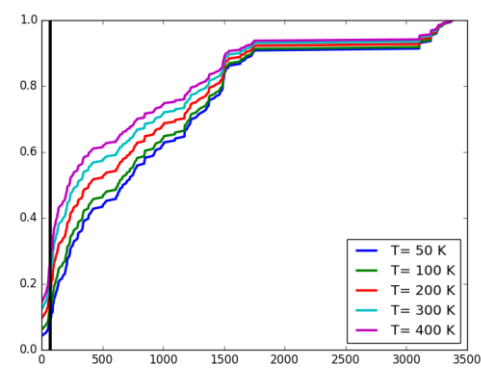
a



b



c



d

Figure S6. Contribution of given frequency to Uiso for Y and W (a) and (b), cumulative contribution of frequencies to Uiso for Y and W (c) and (d).

References

Cliffe, M. J. & Goodwin, A. L. (2012). *J. Appl. Crystallogr.* **45**, 1321–1329.